

Ordered porous polymer films via phase separation in humidity environment

Liang Cui, Juan Peng, Yan Ding, Xue Li, Yanchun Han*

State Key Laboratory of Polymer Physics and Chemistry, Changchun Institute of Applied Chemistry, Chinese Academy of Sciences, Graduate School of the Chinese Academy of Sciences, 5625 Renmin Street, Changchun 130022, People's Republic of China

Received 12 November 2004; received in revised form 25 March 2005; accepted 10 April 2005

Available online 29 April 2005

Abstract

A transition of morphology from island-like structure to disordered and ordered holes on the surface of polystyrene (PS) and poly(2-vinylpyridine) (PVP) blend films were observed with the increase of humidity. At appropriate weight ratio of PS/PVP and PS molecular weight, when humidity reached to a critical value, the hexagonal arrays of holes formed for PS/PVP blend films due to 'breath figures' stabilized by PVP with its strong hygroscopic characteristics during phase separation.

© 2005 Elsevier Ltd. All rights reserved.

Keywords: Ordered porous films; Phase separation; Breath figures

1. Introduction

Ordered macroporous materials have attracted much recent attention because of their potential optical properties such as photonic bandgaps and optical stop-bands [1–3]. Those with pore sizes on the order of micrometers are also of interest for applications in catalysis, sensors, size- and shape-selective separation media, adsorbents, and scaffolds for composite material synthesis [4–6]. Usually, for the preparation of micro-porous materials, the ordered alignment of a template around which the material of interest assembles is required. These templating methods include using block copolymers [7], colloidal crystals [8], emulsions [9], polymers with rod-coil structure [10] and so on. In all cases, structures with sub-micrometer dimensions are prepared, although the use of block copolymer requires an additional step to remove the template. When using colloidal crystal templating, a fluid fills and solidifies in the vacant space between the colloidal crystals. Then, the spheres are removed by solvent extraction or other techniques leaving behind a solid skeleton containing a 3D array of pores. It is obvious that the dimensions of pores

match those of the spheres and cannot be controlled dynamically. The drawback of the emulsion method is that it requires a fractionation procedure to assure the uniformity of the droplet size.

Recently, a simple method that utilizes the condensation of monodisperse water droplets on polymer solution is used to prepare honeycomb macroporous films as pioneered by François et al. [11–14]. The preparation method consists of evaporating a layer of solution spread on a flat support under a flow of moist gas. When solvent and water droplets evaporate completely, an ordered honeycomb array of holes is formed in the solid polymer surface. They found the honeycomb morphologies were obtained with polystyrene block copolymers, star-like homopolystyrenes and linear polystyrenes with a polar terminal group. These polymers self-organized into spherical-shaped structure in carbon disulfide, which was believed to be a determinant element in the formation process. Subsequently, Srinivasrao et al. [15] further investigated this method and prepared 2D and 3D ordered macroporous layers depending on the solvent density with respect to the density of water. They also gave a vivid model for the formation of the regular structure based on thermocapillary convection. Shimomura et al. [16–23] photographed the dynamical movement of the rearrangement of water droplets during honeycomb pattern formation and used different kinds of compounds including organic–inorganic hybrid materials, amphiphilic

* Corresponding author. Tel.: +86 431 5262175; fax: +86 431 5262126.
E-mail address: ychan@ciac.jl.cn (Y. Han).

copolymers, metalorganic, saccharide-containing polymers for patterning. Additionally, two kinds of substrates (solid glass slide and water surface) were used to prepare different porous films. Highly functionalized ordered microarrays of nanoparticles were also developed by ‘breath figures’ [24,25]. Recently, Kim et al. [26] fabricated breath figure patterns on a homopolymer film by spin coating. In addition, they observed that breath figure patterns were generated even when a water-miscible solvent such as tetrahydrofuran (THF) was used as a solvent.

In our previous work, the formation mechanisms and influencing factors on the regular holes pattern in homopolymer films by water droplets templating were studied [27,28]. Immiscible polymer blends can exhibit various morphologies and properties that cannot be provided by a single polymer [29,30]. This paper is another example in which polymer blend films are microstructured into an hexagonal array by ‘breath figures’ and phase separation. Blends of polystyrene (PS) and poly(2-vinylpyridine) (PVP) were selected as the model system since, they have very different chemical characters. The transition of topographies from the island-like to holes was observed with the increase of humidity. After the humidity reached to a critical value, periodically ordered porous films were produced. Humidity, weight ratio of PS/PVP and PS molecular weight played an important role in the formation of the regularly ordered holes.

2. Experimental section

2.1. Materials

Polystyrene (PS-1, PS-2) and poly(2-vinylpyridine) (PVP) were purchased from Aldrich Chemical Company. Polystyrene (PS-3) was obtained from Nanjing University, China. Their characteristics are shown in Table 1. Tetrahydrofuran (THF) (99%, anhydrous) was from Beijing Chemical, China and used without purification.

2.2. Film preparation

The solutions of different weight ratios of PS to PVP at a concentration of 4 wt% in THF were cast onto the cleaning mica substrates by micro-injector. The polymer solutions were filtered with a 0.22 μm millipore membrane before casting. The film thickness was determined by controlling

the volume of solution. Then the mica substrate was put into a vessel plugged with a cork. There are two exhaust pipes on the cork. One opens into atmosphere, the other one is connected with vacuum water pump. Humidity and temperature were measured by hygrothermograph. Solvent evaporation rate was controlled by the air-flowing rate.

2.3. Observation of film morphology

Atomic force microscopy (AFM) measurements were performed on SPA300HV with an SPI 3800 controller, Seiko instruments industry, Co. Ltd. The topographical images were taken with contact mode at room temperature. The tip type was SN-AF01, made of Si_3N_4 . The scan rate was about 1.0 Hz and the applied force was remained at the minimal value in order to keep the contact between the tip and sample. The overall phase domain morphology was determined by selective dissolution of PVP-rich phase for the films immersed for 3 min in ethanol.

3. Results and discussion

3.1. The influence of humidity on the formation of ordered macroporous films

Fig. 1(a)–(f) indicated the changes of the film surface topographies of PS-2/PVP (5/1) (w/w) cast from THF solution (4 wt%) onto the mica substrate at different humidity with the air flow rate of 0.2 l/min. The film thickness was ca. 0.3 μm . In case of 10% ambient humidity (Fig. 1(a)), the island-like domains were distributed on the film surface. When the humidity increased to 15%, some holes and islands emerged simultaneously (Fig. 1(b)). Moreover, when the humidity increased to 25%, disordered isolated holes were distributed on the surface (Fig. 1(c)). When the humidity was over 30%, a 2D ordered porous film with uniform size formed (Fig. 1(d)–(f)). The inset of Fig. 1(d) indicated a perfect hexagonal arrangement of the holes by fast Fourier transform (FFT) pattern. In addition, the sizes and the depth of the holes with uniformity on the surfaces increased with the increase of humidity, i.e. from 2.3 μm , 250 nm (Fig. 1(d)), increased to 3.4 μm , 650 nm (Fig. 1(e)), and 4.0 μm , 730 nm (Fig. 1(f)).

In order to get insight into the morphology evolution process, it is necessary first to make clear the composition of the polymer films. Fig. 1(a') and (b'), corresponding to Fig. 1(a) and (b), respectively, were the images after the PVP-rich phase was dissolved by ethanol, a good solvent for PVP. It can be seen that the holes were left on the film surface, which indicated that minor domains on the film surface in Fig. 1(a) and (b) were PVP. The sample of Fig. 1(c) was also immersed in ethanol. There was no obvious change of the surface morphology (Fig. 1(c')). However, the depth of the holes changed from 90 nm before the film was dissolved by ethanol (the thickness of the film

Table 1
Characteristics of PS and PVP

Polymer	M_w (K)	M_n (K)	M_w/M_n
PVP	11	9.5	1.15
PS-1	11	10.6	1.03
PS-2	212	200	1.06
PS-3	582	522	1.11

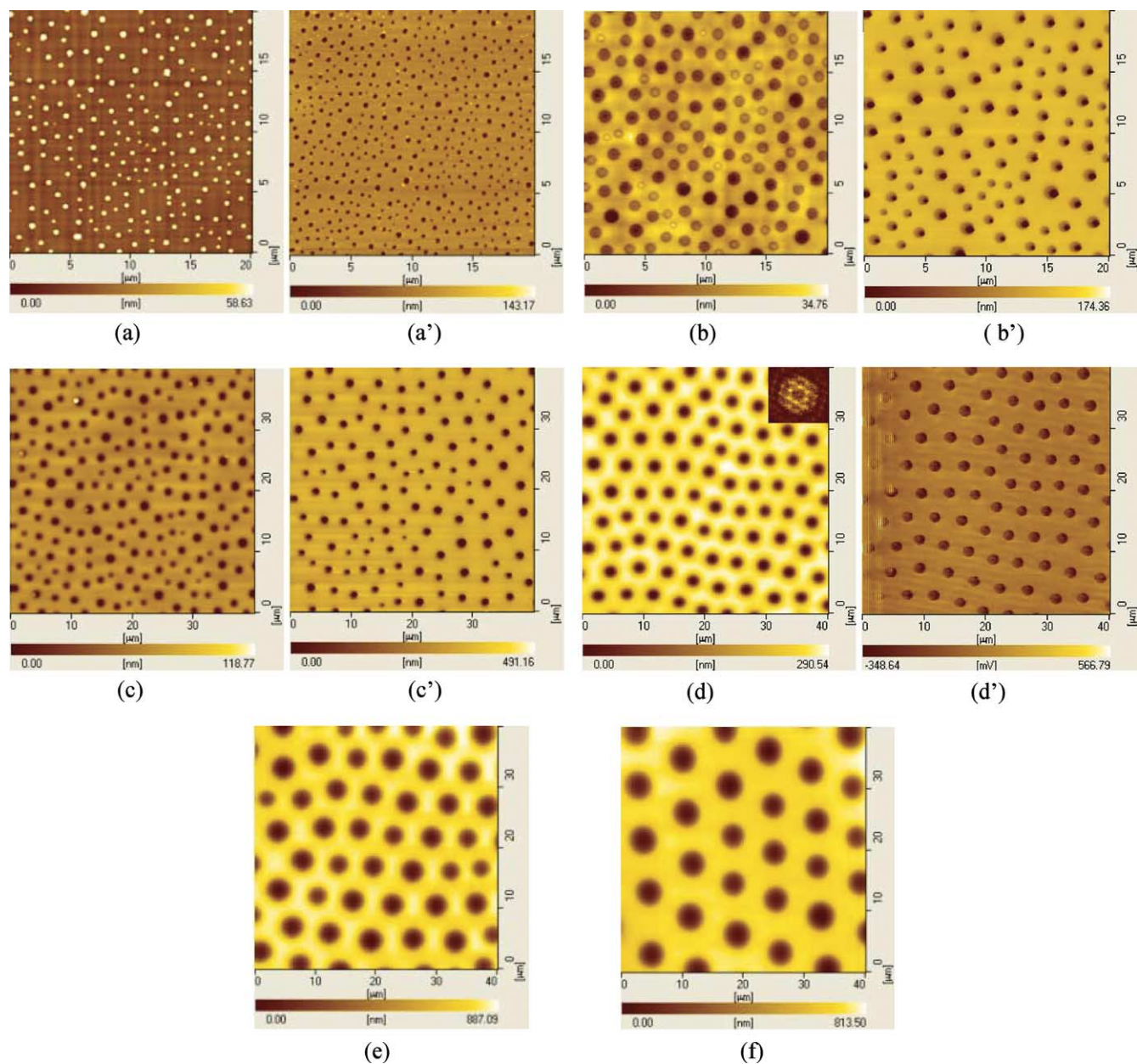


Fig. 1. The morphology evolution of film surfaces for PS-2/P2VP (5:1) cast from THF solution at a concentration of 4 wt% in different humidity. The humidity is (a) 10%; (b) 15%; (c) 25%; (d) 30%, (e) 50%; (f) 70%, respectively. (a')–(c') are the AFM topographic images corresponding to (a)–(c) respectively, after removal of the PVP dissolved by ethanol. The image (d') is the frictional image of (d). The inset in (d) is the result of 2D fast Fourier transforms (FFT) analysis of the height fluctuations.

was about $2.2 \mu\text{m}$) to 550 nm after the PVP was removed. It showed that PVP phase was situated inside the holes and these holes were not through to the substrate. Meanwhile, the frictional image of the same area showed that the properties inside and outside of the holes were quite different (Fig. 1(d) and (d')). The bright parts were corresponding to PS-rich phase and the dark parts corresponding to PVP-rich phase according to the different properties of PVP and PS.

Krausch et al. [31] reported the upthrust of PVP-rich phase in thin PS/PVP films by spin coating from THF solution in air. The author attributed this effect to the

different solubility of the two polymers in their common solvent. THF is a better solvent for PS than that for PVP. The PVP-rich phase should more quickly deplete of the solvent and turn solid earlier than the PS phase, i.e. the PVP phase should protrude from the PS background. In case of 10% ambient humidity (Fig. 1(a)), the minority of islands-like PVP-rich phase distributed on the continuous PS phase surface resulting from the PVP concentration was sharply less than PS concentration in THF solution (PS:PVP (w/w)=5:1). However, when the humidity increased, the islands of PVP-rich phase changed into pits. The humidity is

the critical factor for morphologies transition. It is well known that PVP has strong hygroscopic character. The solvent evaporation decreased the temperature of the solution surface, and then water vapor would condense onto it, leading to formation of water droplets [11–15]. In our previous work, the formation of water droplets on the surface of polymer solution during the solvent evaporation was observed by optical microscopy when toluene (immiscible with water) was used as the solvent. While THF (miscible with water) was employed as the solvent, there were no holes on the film surface due to water droplets dissolving into solvent [28]. In contrast to homopolymer, in PS/PVP blend system, even when a water-miscible solvent such as THF was used as a solvent, hole patterns were generated since the water droplets were taken and stabilized by PVP due to its strong hygroscopic characteristics when phase separation occurred. Because the water droplets were protected by PVP, they could not contact with the solvent. The PVP absorbing water would sink into the PS matrix due to the gravity. After the water evaporated, elevated islands were substituted by concave holes (Fig. 1(c)–(f)). The islands with pits in Fig. 1(b) emerged resulting from the water droplets partly occupied the PVP-rich islands due to the low humidity. A strong linear correlation between the atmospheric humidity and pores sizes has been reported [26,28]. Higher humidity resulted in larger pores. Similarly, in this work, the sizes of the holes increased with the increase of the humidity due to coalescence of water droplets.

Further, why did the ordered porous film emerge when the humidity reached over 30%? When the water vapor condensed onto the cold film surface due to solvent evaporation, it appeared in the form of drops, known as ‘breath figures’. It has been widely studied and used to micropattern thin films. Monodisperse droplets can arrange in a hexagonal arrangement and acts as a template around which the polymer assembles. The water droplets are stabilized by the polymer is the critical factor for breath figure patterns. The PS and PVP have very different chemical characters (the water contact angle of PS and PVP is 90° and 50°, respectively). Polar PVP-rich phase particles floated upward due to phase separation and moved to the water-droplets by an attractive interaction between water droplets and PVP. The attractive interaction was due to the strong hygroscopic character of PVP. These PVP-rich phase particles distributed randomly and isolate on the film surface under low humidity. When the humidity reached to a critical value, more and more water droplets formed on the solution surface. These water droplets attracted each other in a much stronger way than the single water droplet because the attractive force between the droplets was proportional to the sixth power of that between the single water droplet [32]. But these condensed water droplets were prevented due to stabilization by PVP and the existence of hydrophobic PS layer. In addition, the phase separation of PS and PVP presented weak repulsive capillary forces between the water droplets. The equilibrium between the

attracted force and repulsive capillary forces led to the droplets in arranged locally a well-ordered packing [33]. When the system reaches the equilibrium conditions, the preferred packing arrangement of the spherical microdomains will be that which corresponding to the lowest free energy [34]. For thin films containing only a single layer of droplets, the hexagonal arrangement provides the lowest free energy. The close adjacent droplets are attracted to each other and repulsed by the lateral capillary force, which causes the dense hexagonal packing. Therefore, ordered porous film emerged when the humidity reached over 30%.

From the above results, it can be concluded that the formation of the porous film originated from the increase of the ambient humidity and strong hygroscopic character of PVP during the phase separation. To further demonstrate the porous film formation mechanisms, we observed the reversible transition of surface morphologies over time after the porous films were put into water (Fig. 2(a)–(d)). Fig. 2(a) was the image formed at the same condition as that in Fig. 1(c). Island-like structure appeared when the sample was dipped in water for 20 min (Fig. 2(b)). Then, the islands became larger after immersed in water for 2 h (Fig. 2(c)). When the film was dried, the holes recovered completely as the original topography (Fig. 2(d)). This reversible morphology transition further demonstrated that the PVP-rich phase domains were inside the holes.

Based on the above results, Fig. 3 shows the schematic illustrations for the transition of ordered porous films formation with the increase of humidity. (a) In a low humidity atmosphere, the PVP will more quickly deplete of the solvent and solidify on the surface than the PS owing to the THF is a better solvent for PS than that for PVP. The elevated PVP islands formed due to the solvent evaporation. (b) With increasing the humidity, the solvent evaporation cools the solution surface, leading to the growth of moisture and formation of water droplets. These water droplets are caught by the PVP phase because PVP is more hydrophilic than PS. Although the solvent (THF) is miscible with water, the water droplets are stabilized by PVP islands and cannot be dissolved into solvent. Then, the water drops sink to the solution with random distribution. (c) When the humidity reached to a critical value, more and more water droplets condense onto the solution surface. These close adjacent droplets are attracted to each other and repulsed by the lateral capillary force that causes dense hexagonal packing. The PVP-rich phase islands are arranged by the water droplets. (d) At last, the water droplets and solvent evaporate completely, leaving the regular holes pattern.

3.2. The influence of molecular weight of PS on the formation of ordered pattern

Fig. 4 described the morphologies with different PS molecular weight of PS/PVP (5/1) (w/w) blends at the same condition as that in Fig. 1(e). For PS-3 with higher molecular weight (582k), disordered holes distribution

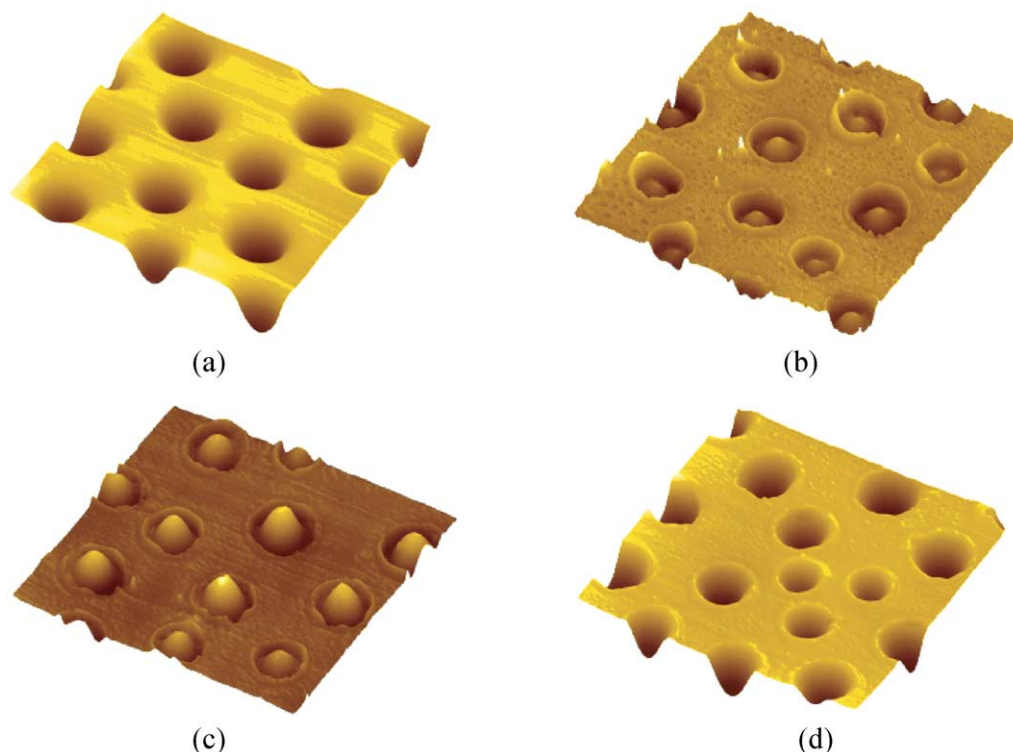


Fig. 2. The 3D restructuring images of the films obtained as the same condition as Fig. 1(c) in water at different times: (a) air; (b) 20 min; (c) 1 h; (d) after drying. The image size is $10 \times 10 \mu\text{m}^2$.

was produced on the film surface (Fig. 4(a)). With the decrease of PS molecular weight to 212k, ordered holes appeared (Fig. 4(b)). However, when the M_w of PS decreased to 11 K, nearly no holes left on the film thereby (Fig. 4(c)). It showed that only in an appropriate range of molecular weight of PS, could the ordered patterns form when casting-solution of PS and PVP in THF evaporated under humid conditions. The solution viscosity determined by molecular weight of polymers [28] and the behavior of phase separation jointly played a role in the formation of ordered patterns.

When PS with high molecular weight was used such as PS-3 and PS-2, the difference between the M_w of PVP and PS increased so that it led the phase-separation to take place far from symmetry system [35]. The island-like structure of PVP-rich phase formed when solvent concentration reached to the critical point of phase separation due to the solvent evaporation. The PVP with strong hygroscopic character like a surface-active compound stabilized the water droplets in despite of the high viscosity. However, too high viscosity due to high M_w (e.g. PS-3) was not helpful for the ability of PVP-rich phase domains movement. The attracted force between water droplets was not enough to overcome the movement resistance of PVP-rich phase domains. Therefore, PVP-rich phase domains could not be well rearranged by the water droplets templates. The holes emerged on the film surface without regularity after complete evaporation of the solvent. When PS with 11 K was used, the difference

between the M_w of PVP and PS reduced and the viscosity decreased. The movement ability of PVP phase increased. PVP-rich phase domains were easy to aggregate and form into continuous phase. Moreover, the coalescence of water droplets stabilized by PVP phase could not be prevented due to lower solution viscosity determined mainly by PS. Thereafter, these water droplets condensed into continuous phase that distributed on the film surface. A film with surface undulation formed after the complete evaporation of water and solvent. Therefore, only in an appropriate range of molecular weight of PS could the ordered pattern form.

3.3. The influence of weight ratio of PS/PVP on the formation of ordered pattern

The weight ratio of PS/PVP is another factor determining the formation of ordered pattern. Fig. 5(a)–(c) described the images of PS/PVP (5/1) (w/w), (10/1) (w/w) and (20/1) (w/w) blends at the same condition as that in Fig. 1(d). With increasing the weight ratio of PS/PVP, the regularity of holes decreased. In addition, the sizes and the surface fraction of the holes on the surfaces decreased with the increase of the weight ratio of PS/PVP, i.e. from 2.3 μm , 14.6% (Fig. 5(a)), decreased to 1.0 μm , 9.2% (Fig. 5(b)), and 0.85 μm , 6.3% (Fig. 5(c)).

The influence of composition of polymer blends on the phase separation behavior has been studied [36]. The weight ratio of PS/PVP influenced the distribution of phase

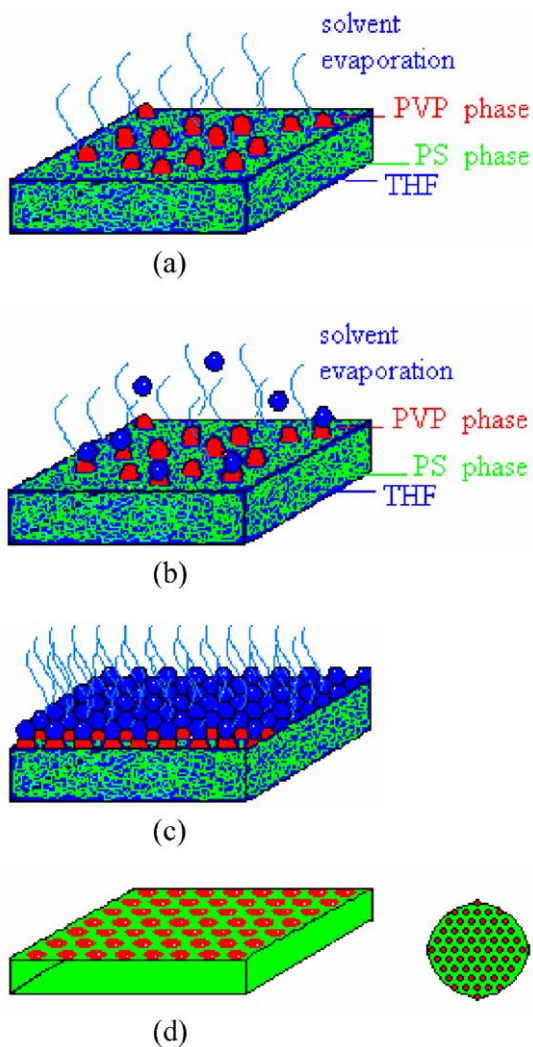


Fig. 3. The schematic illustrations for the process of a casting solution with solvent evaporation at different humidity.

domains on the film surface due to phase separation. The decrease of PVP component would lead to decrease of the density of PVP-rich phase domains, which directly led to the increase of distance between the PVP-rich phase domains. On the other hand, the viscosity increased with the increase of PS component from 5/1(w/w) to 20/1(w/w) (PS/PVP). Therefore, PVP domains could not be well rearranged by the water droplets due to the larger distances between the PVP islands and higher viscosity.

4. Conclusions

The hexagonal arrays of holes could be produced for PS/PVP blend films during phase separation when the humidity reached a critical value. In a lower humid atmosphere, the disordered islands-like pattern or holes distributed on the surface of the films due to the dispersive water droplets stabilized by PVP with strong hygroscopic character during solvent evaporation. In a higher humid environment, the water droplets assembled into hexagonal arrays. The PVP domains were reassembled by the water droplets template. Thus, the ordered holes were formed after solvent and water evaporated. The influence of molecular weight of PS and weight ratio of PS/PVP on the formation of the ordered pattern reflected that the viscosity and the behavior of phase separation played an important role in the formation of ordered patterns. Only in an appropriate range of molecular weight of PS and weight ratio of PS/PVP could the ordered pattern form.

Acknowledgements

This work is subsidized by the National Natural Science Foundation of China (50125311, 20334010, 20274050, 50390090, 50373041, 20490220, 20474065, 50403007), the Ministry of Science and Technology of China

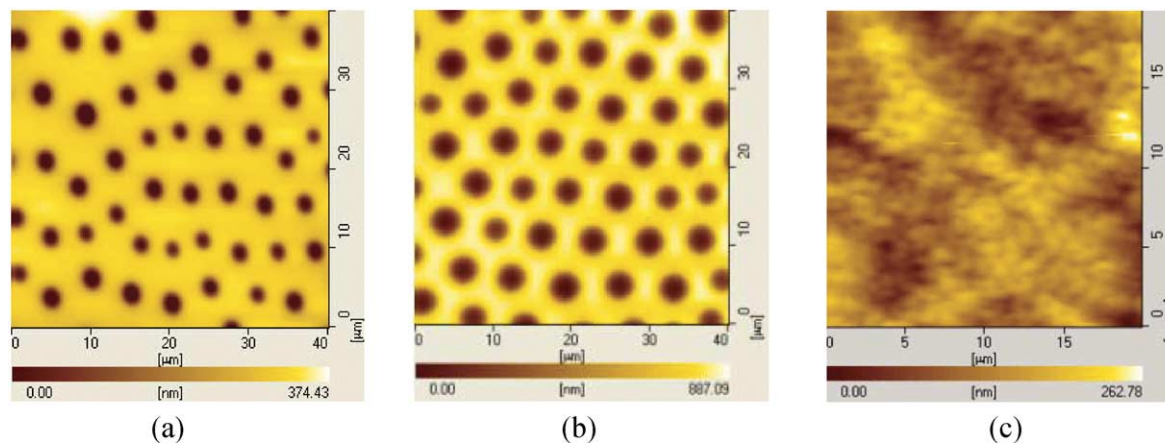


Fig. 4. (a)–(c) The topographic images of different molecular weight of PS for PS/P2VP (5/1) (w/w) blend films cast from THF solution at a concentration of 4 wt% in 50% humidity. The molecular weight of PS is (a), 582 K; (b), 212 K; (c), 11 K, respectively.

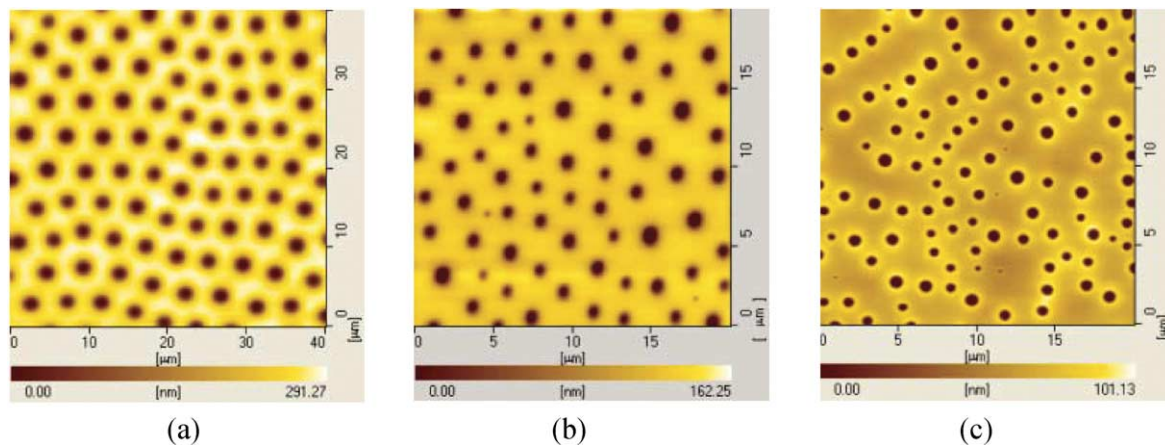


Fig. 5. The topographic images for different weight ratios of PS-2/P2VP blend films cast from THF solution at a concentration of 4 wt% in 30% humidity. (a) 5/1; (b) 10/1; (c) 20/1.

(2003CB615601), the Chinese Academy of Sciences (Distinguished Talents Program, KJCX2-SW-H07) and the Jilin Distinguished Young Scholars Program (20010101).

References

- [1] Yablonovitch E. *J Opt Soc Am B* 1993;10:283.
- [2] Joannopoulos JD, Meade RD, Winn JN. *Photonic crystals: molding the flow of light*. Princeton, NJ, USA: Princeton University Press; 1995.
- [3] Soukoulis C. *Photonic band gap materials*. Dordrecht: Kluwer; 1996.
- [4] Tanev PT, Chibwe M, Pinnavaia TJ. *Nature* 1994;368:321.
- [5] (a) Kresge CT, Leonowics ME, Roth WJ, Vartuli JC, Beck JS. *Nature* 1992;359:710.
(b) Zhao DY, Feng JL, Huo QS, Melosh N, Fredrickson GH, Chmelka BF, et al. *Science* 1998;279:548–52.
(c) Krämer E, Förster S, Göltner C, Antonetti M. *Langmuir* 1998;14:2027.
- [6] Wijnhoven JEGJ, Vos WL. *Science* 1998;281:802.
- [7] Li Z, Zhao W, Liu Y, Rafailovich MH, Sokolov J. *J Am Chem Soc* 1996;118:10892.
- [8] Velev OD, Jede TA, Lobe RF, Lenhoff AM. *Nature* 1997;389:447.
- [9] Imhof A, Pine DJ. *Nature* 1997;389:948.
- [10] Jenekhe SA, Chen XL. *Science* 1999;283:372.
- [11] Widawski G, Rawiso B, François B. *Nature* 1994;369:387.
- [12] Pitois O, François B. *Eur Phys J B* 1999;8:225.
- [13] François B, Pitois O, François J. *Adv Mater* 1995;7:1041.
- [14] Pitois O, François B. *Colloid Polym Sci* 1999;277:574.
- [15] Srinivasarao M, Collings D, Philips A, Patel S. *Science* 2001;292:79.
- [16] Maruyama N, Koito T, Nishida J, Sawadaishi T, Cieren X, Ijio K, et al. *Thin Solid Films* 1998;327–329:854.
- [17] Karthaus O, Cieren X, Maruyama N, Shimomura M. *Mater Sci Eng, C* 1999;10:103.
- [18] Nishikawa T, Nishida J, Ookura R, Nishimura SI, Wada S, Karino T, et al. *Mater Sci Eng, C* 1999;10:141.
- [19] Nishikawa T, Nishida J, Ookura R, Nishimura SI, Wada S, Karino T, et al. *Mater Sci Eng, C* 1999;8–9:495.
- [20] Karthaus O, Maruyama N, Cieren X, Shimomura M, Hasegawa H, Hashimoto T. *Langmuir* 2000;16:6071.
- [21] Nishikawa T, Ookura R, Nishida J, Arai K, Hayashi J, Kurono N, et al. *Langmuir* 2002;18:5734.
- [22] Nishikawa T, Nonomura M, Arai K, Hayashi J, Kurono N, Sawadaishi T, et al. *Langmuir* 2003;19:6193.
- [23] Yabu H, Tanaka M, Ijio K, Shimomura M. *Langmuir* 2003;19:6297.
- [24] Böker A, Lin Y, Chiapperini K, Horowitz R, Thompson M, Carreon V, et al. *Nat Mater* 2004;3:302.
- [25] Shah PS, Sigman Jr MB, Stowell CA, Lim KT, Johnston KP, Korgel BA. *Adv Mater* 2003;15:971.
- [26] Park MS, Kim JK. *Langmuir* 2004;20:5347.
- [27] Peng J, Han YC, Fu J, Yang YM, Li BY. *Macromol Chem Phys* 2003;204:125.
- [28] Peng J, Han YC, Yang YM, Li BY. *Polymer* 2004;45:447.
- [29] Bates FS. *Science* 1991;251:898.
- [30] (a) Ray SS, Pouliot S, Bousmina M, Utracki LA. *Polymer* 2004;45:8403.
(b) Li YJ, Shimizu H. *Polymer* 2004;45:7381.
(c) Akiba I, Masunaga H, Sasaki K, Shikasho K, Sakurai K. *Polymer* 2004;45:5761.
(d) Liu SY, Chan CM, Weng LT, Jiang M. *Polymer* 2004;45:4945.
- [31] Böltau M, Walheim S, Mlynek J, Krausch G, Steiner U. *Nature* 1998;391:877.
- [32] Chan DYC, Henry Jr JD, White LR. *J Colloid Interface Sci* 1981;79:410.
- [33] Pitois O, François B. *Colloid Polym Sci* 1999;277:574.
- [34] Thomas EL, Kinning DJ, Alward DB, Henke CS. *Macromolecules* 1987;20:2934.
- [35] Li X, Xing RB, Zhang Y, Han YC, An LJ. *Polymer* 2004;45:1637.
- [36] Budkowski A, Bernasik A, Cyganik P, Raczowska J, Penc B, Bergues B, et al. *Macromolecules* 2003;36:4060.